Available online at www.sciencedirect.com

ScienceDirect

Energy Procedia 137 (2017) 214–222

Energy Procedia

www.elsevier.com/locate/procedia

14th Deep Sea Offshore Wind R&D Conference, EERA DeepWind'2017, 18-20 January 2017, Trondheim, Norway

Wind Tunnel Wake Measurements of Floating Offshore Wind Turbines

I.Bayati*[a], M.Belloli[a], L.Bernini[a], A.Zasso[a]

[a]*Politecnico di Milano, Dipartimento di Meccanica, Via La Masa 1, 20156, Milano, Italy*

Abstract

This paper reports the results of a wake measurement campaign carried out at Politecnico di Milano wind tunnel to support current studies of the authors about unsteady aerodynamics of floating offshore wind turbines (FOWT) as well as evaluating experimental evidence for wind farm applications of FOWT. The wind turbine scale model adopted for these tests is the 1/75 DTU 10 MW wind turbine developed for the LIFES50+ project. In this study, imposed surge motions, at different frequencies and amplitudes, were provided at the base of the turbine's tower, to investigate the influence of motion on the wake. Results reported show good agreement with the state-of-the-art of wind turbines wake aerodynamics in steady conditions; concerning the unsteady conditions (imposed motion) interesting data are reported and collected with respect to a "wake reduced frequency" parameter which is, according to the authors, a straightforward value to estimate the "level" of unsteadiness connected to a specific dynamic condition due to floating motion. Interesting and consistent phenomena are observed and commented, although opening to the need of further experimental and numerical investigations.

Peer-review under responsibility of SINTEF Energi AS.

Keywords: Floating Offshore Wind Turbines, FOWT, Wake, Unsteady Aerodynamics, Wind Farm

1. Introduction

As Floating Offshore Wind Turbines (FOWT) are currently attracting great interest from scientific and industrial sectors, the importance of investigating thoroughly the aerodynamics of such system, which is made more complex due to the motion of the platform, is evident. The unsteady aerodynamics, which is a characteristic of FOWTs, is still far from being extensively understood, and this has an impact on the optimization of their design and power production. Furthermore, the comprehension of the wake behaviour downstream of a FOWT, is fundamental in wind farm application (e.g. optimal layout and control), and literature of this topic is still scarce, compared to onshore application ([1],[2]). This paper aims at reporting a first set of wake measurements, carried out downstream of a

* Corresponding author. Tel.: +39-02-2399-8486 ; fax: +39-02-2399-8202.
E-mail address: ilmasandrea.bayati@polimi.it

1876-6102
Peer-review under responsibility of SINTEF Energi AS.
10.1016/j.egypro.2017.10.375

1/75 wind turbine scale model ([3], [4]), in imposed surge motion conditions, at difference amplitudes, frequencies and wind turbine operational conditions, with the goal of providing a first reference in the assessment of the wake of FOWTs. This was also performed to support the current assessment of unsteady aerodynamics of wind turbines that authors are carrying out, based on experimental evidences coming from the same experimental setup (Fig.1) imposing surge and pitch motions ([5], [6]), in the same facility (Politecnico di Milano, 14x4 m Atmospheric Boundary Layer Wind Tunnel).

Although the literature in this topic is weak, previous studies are worth mentioning, as [7], where a model floating wind turbine was assembled on a TLP structure and installed in a wind tunnel and water tank respectively: near wake measurements were carried out using single probe hot wire anemometry for both fixed and floating platform conditions, at fixed distances downstream of the rotor under floating conditions. It was found that for higher tip speed ratios (λ) greater difference in the aerodynamic performances (e.g. C_P) were evident. This was also confirmed by numerical studies in [8] and [9], which concluded that the difference between the mean power coefficient under platform surge conditions and the steady power coefficient depends either on platform surge frequency, surge amplitude and the rotor operating conditions. Furthermore, in [10] experiments were performed using two model wind turbines operated in tandem with a bottom-fixed configuration and a floating configuration with both turbines allowed to freely oscillate in the stream- wise direction. Wakes of both turbines were measured using stereoscopic Particle Image Velocimetry (PIV) concluding that the pitching motion of the turbine leads to the need of longer distances between floating turbines in a farm, to allow for a better recovery of the wake to achieve the same power production, as for bottom fixed turbines.

In the present paper a traversing system with a hot-wire anemometer was adopted for carrying out downwind air velocity measurements at a fixed distance from the turbine (2.3 times the diameter D), for different operational conditions (below-, above- and rated) as well as for different amplitudes and frequencies of the imposed surge motions, spanning a range considered significant for a floating wind turbines of such size (10 MW).

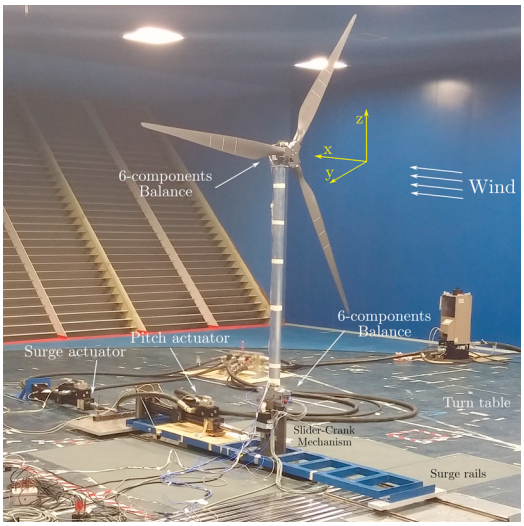

Fig. 1: Wind tunnel setup

2. Wind tunnel tests

2.1. Wind turbine model and setup

The wind turbine model used for this work is a scaled model of the DTU 10MW reference wind turbine [11]. It has been designed by the authors ([3], [12], [13]) as part of the LIFES50+ EU H2020 project [14], which aims at providing cost effective technology for floating substructures for 10 MW wind turbines through a novel approach in

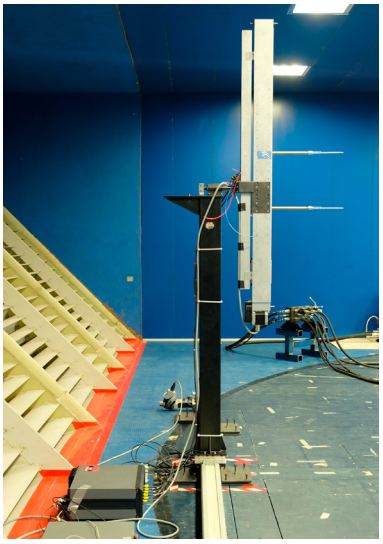

Fig. 2: Hot-wire anemometers mounted on the traversing system, downwind the wind turbine, for wake measurements

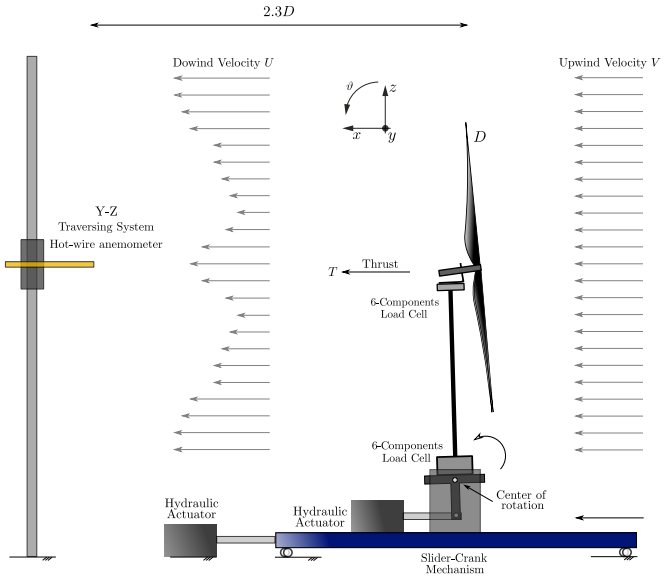

Fig. 3: Sketch of the wind tunnel setup and conventions

wind tunnel and ocean basin testing for offshore wind energy (i.e. hybrid/HIL, [15], [16], [17] and [18]). The main specifications are reported in Tab. 1 where the length λ_L and velocity λ_V scales were chosen in order to optimize the model performance with respect dimensions and wind speed range of Politecnico di Milano wind tunnel, [19]. Further information on the scaling approach can be found in ([4], [13]).

Since the aim of this work is the analysis of the unsteady aerodynamics due to the motion of the floating platform, the 2 degrees-of-freedom described in [5] was adopted, which is suitable to imposed the motion, along surge and pitch, to the wind turbine scale model, by means of an hydraulic system, as in Fig.1. During the wind tunnel tests reported in this work, mono-harmonic imposed sine waves were provided at the base of the tower along surge only direction x. As it can be seen in Fig. 3, the test rig includes two 6-components load cells to measure the forces either at the top and base of the tower. Moreover, a laser sensor was used to measure the actual surge displacement of the turbine.

Table 1: Wind Tunnel Model turbine specifications

Parameter	value	units	scale
Cut in wind speed	1.33	m/s	$\lambda_V = 3$
Cut out wind speed	8.33	m/s	$\lambda_V = 3$
Rated wind speed	3.67	m/s	$\lambda_V = 3$
Rotor Diameter	2.38	m	$\lambda_L = 75$
Maximum Rotor Speed	240	rpm	$\lambda_f = \lambda_L \lambda_V^{-1} = 25$

2.2. Wake measurement system

The wake generated by the wind turbine was measured by an automatic traversing mechanism employing tri-axial sensor probe hot-wire anemometers. The sensors can measure the three wind velocity components with an acceptance cone of approximately 70°. In Fig.2 the traversing system with the mounted hot-wire probes is reported. The traversing

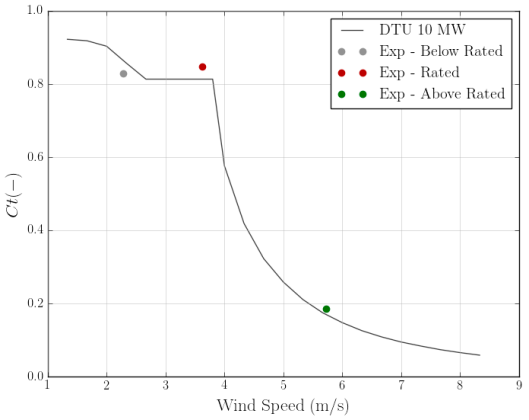

Fig. 4: Thrust coefficient as function of wind speed: full scale target compared to PoliMi model

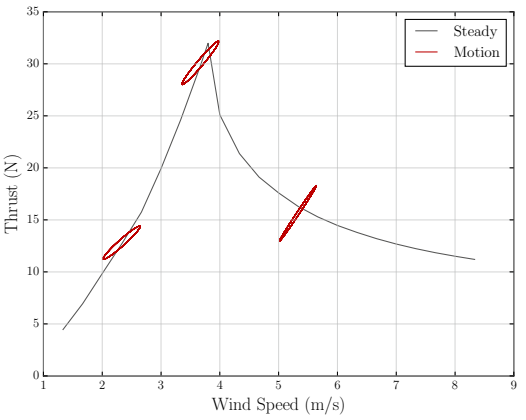

Fig. 5: Unsteady thrust force due to the imposed motion over the static curve

system was placed at 2.3 times the rotor diameter D (2.38 m). This distance was chosen either due to practical issue as well as for investigating wake condition at distance greater than 2D, which is considered the lower limit for near wake region [2]. This allow to draw considerations valid for floating offshore wind farms.

The sampling plane is perpendicular the mean wind speed direction, plane yz in Fig. 3, so that the traversing was capable to move the probe (Fig.2) at any location of the 2.3D plane with the limits $y_{lim} = \pm 1.6m$ and $z_{lim} = 0.5 - 3.5m$. Measurements with and without the surge imposed motion were mainly carried out along the line at hub height ($z = 2.1m$), turning out with 33 point series (i.e. sampling distance of 0.1 m from -1.6 m to +1.6 m) along the cross wind y-direction. Nevertheless, for a single turbine condition, with the machine at rated wind speed and fixed motion platform, a full 2D plane was sampled moving the probe both in the y-direction and in the z-direction (y spacing equal to 0.1, z spacing equal to 0.35 m). At each position the acquisition time was 60 s, with a 2000 Hz sampling frequency.

2.3. Imposed motion

During the wind tunnel tests herein analysed, a series of wind turbine dynamic conditions were tested, over three different wind tunnel speeds: rated wind speed at 3.67 m/s, below the rated at 2.33 m/s and one above the rated at 5.33 m/s, as reported in Tab.2. These tree conditions were chosen as representative of all the possible wind condition normally encountered by the turbine in operation, in aerodynamic sense. A smooth inflow condition were always considered, with a background turbulence intensity of approximately 2%. Either the rotational speed and blade pitch were kept fixed at the corresponding nominal values during the tests (e.g. neither main shaft control below rated or collective pitch control above rated). In Fig.4 the model thrust coefficient compared to the target full scale one, is reported: it is worth noticing that this very good agreement is of extreme importance since the far wake properties are mainly function of the thrust generated by the turbine ([1], [2]), this make the results reliable. More details of the consistent aerodynamic design of the wind turbine model can be found in [4] and [12].

The wake at the three tested wind speeds was sampled either considering the turbine fixed or imposing a sinusoidal surge motion, by different combinations of amplitudes and frequencies, Tab.2, which can be linked to low- and wave-frequency motions at full scale, although this study is to asses the unsteady aerodynamics independently. Nevertheless, the unsteady aerodynamics, according to the authors [6] can be well represented by a non-dimensional parameter, the "wake reduced velocity" V_W^*, which is function of the incoming wind speed U_∞ the frequency of motion f and the rotor diameter D, as

$$V_W^* = \frac{U_\infty}{f \cdot D} \tag{1}$$

Therefore, the wake reduced velocity V_W^* can be considered as the number of rotor diameters D travelled by a reference air particle drifted by the undisturbed wind speed U_∞ within one cycle of surge platform's motion at frequency f. So

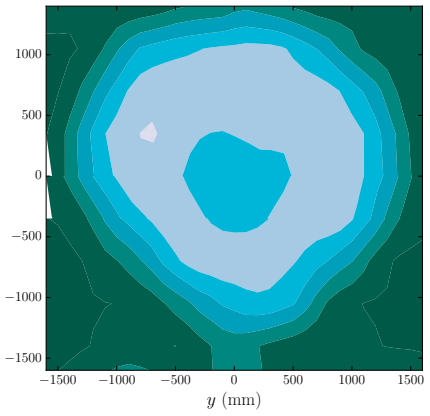

Fig. 6: 2D map of the downwind velocity at rated wind

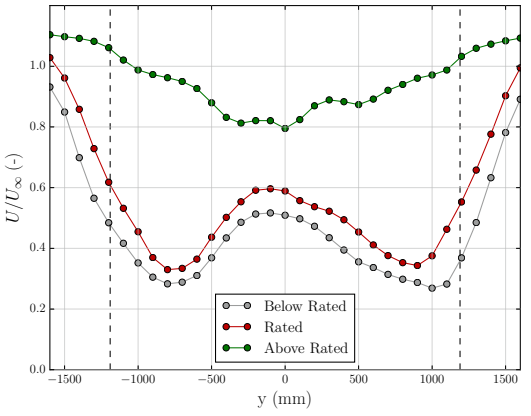

Fig. 7: Wake deficit, at hub height and 2.3D, for below rated, rated and above rated conditions. Dashed vertical lines for the blade tip position along y axis

V_W^* is indicative of the aerodynamic unsteadiness due to the wind turbine rotor that re-enters its own generated wake for low values of V_W^*. On the contrary, for higher values of V_W^* quasi-steady theory can be applied to the aerodynamics of FOWTs, as from recent experimental and numerical studies by the authors, [5] and [6]. This interpretation seems to be consistent, based on the following results, however it certainly requires further experimental/numerical comparison and investigation.

Full Scale			**Wind Tunnel**			V_W^*
U (m/s)	Amp x_0 (m)	Period T (s)	U (m/s)	Amp x_0 (m)	Frequency f (Hz)	(-)
7	7.5	100	2.3	0.1	0.25	≈ 4
	2.25	25		0.03	1	≈ 1
	1.125	12.5		0.015	2	≈ 0.5
11	7.5	100	3.6	0.1	0.25	≈ 6
	2.25	25		0.03	1	≈ 1.5
	1.125	12.5		0.015	2	≈ 0.8
16	7.5	100	5.3	0.1	0.25	≈ 9
	2.25	25		0.03	1	≈ 2.2
	1.125	12.5		0.015	2	≈ 1

Table 2: Surge imposed motion test matrix

3. Results

In Fig 6 the map of the wake velocity U measured at rated wind speed it is reported normalized over the undisturbed incoming wind flow U_∞. This measurement was mainly to verify the correctness and the consistency of the measurements that will be reported in the following, by carrying out a more comprehensive measurement on the whole plane at 2.3D downwind distance (Fig.3). Therefore, the thrust force was computed given the measured wake deficit and compared to the direct thrust measurement of the 6-component balance, which bears the whole wind turbine rotor (Fig. 1 and 3). More specifically, defining U_∞ and U respectively as the undisturbed wind speed and the measured along-wind wake velocity, the thrust force T can be computed as:

$$T = \int_A U(U_\infty - U)\rho dA \tag{2}$$

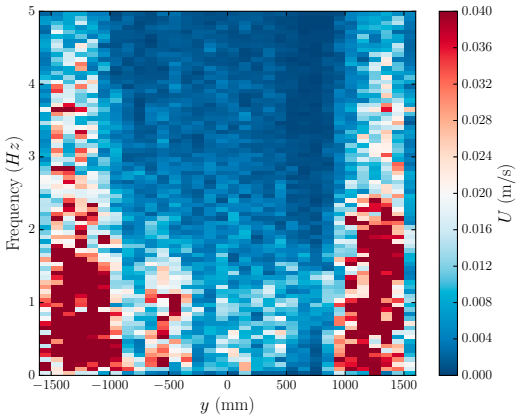

Fig. 8: Spectrogram of the along wind wake velocity U with steady wind condition (no imposed surge motion) at rated wind speed

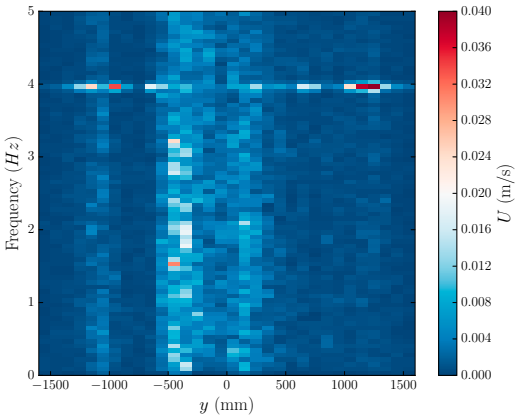

Fig. 9: Spectrogram of the along wind wake velocity U with steady wind condition (no imposed surge motion) at above-rated wind speed

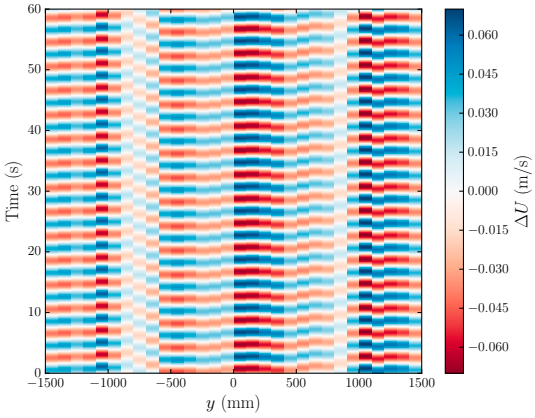

Fig. 10: Along wind wake velocity U with imposed surge motion at $f = 0.25$ Hz at rated wind speed

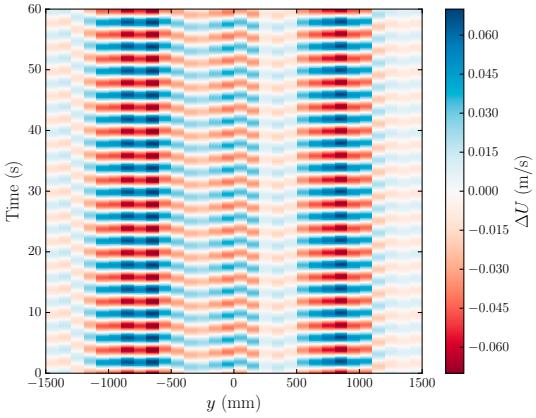

Fig. 11: Along wind wake velocity U with imposed surge motion at $f = 0.25$ Hz at above-rated wind speed

where A is the deficit area considered for the integration of the wake velocity U: it was chosen an area A contained in a circumference of radius 1400 mm. Both the direct force measurement and the wake deficit integration (Eq.2) gave the same result at rated wind speed (Fig. 4 and 5), confirming the correctness of the experimental setup and measuring system. For all the other measurements, with and without the surge imposed motion, only the wake velocity at hub height was measured, as explained in details in the section 2.2.

In Fig.7 the wake deficits in steady conditions (no motion) are reported for below-, rated and above-rated wind condition (see 4). As expected from literature ([1], [2]), the aerodynamic efficiency (4) plays an important role in the downwind velocity field. Therefore, it is evident that the below-rated and rated conditions, which have nearly the same thrust coefficient C_t (Fig.4), are characterized by almost the same shape and entity of the wake velocity, whereas for the above rated condition, characterized by a significantly lower thrust coefficient, has a greatly lower wake deficit with a completely different distribution along the cross-wind (y) direction at hub height.

Also the turbulence intensity characterizing the wake is strictly connected to the entity of power extraction of the rotor from the incoming wave, and this is, in turn, given by the related thrust coefficient C_t ([20]). This is clearly visible from Fig.8 and 9, for steady conditions, respectively at rated and above-rated conditions. It is evident how in Fig.8 the greater turbulence distribution along the cross-wind direction, with a higher smearing around the blade

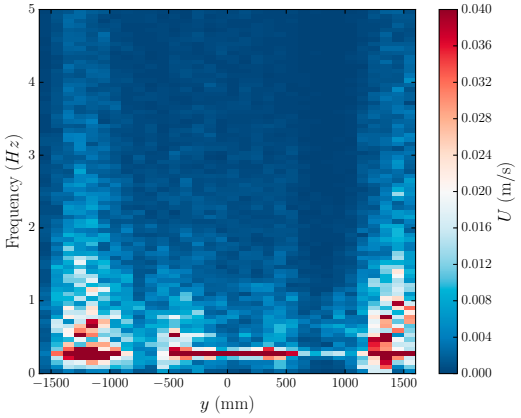

Fig. 12: Spectrogram of the along wind wake velocity U, with imposed surge motion with wake reduced velocity $V_W^* = 4$, at below-rated wind speed

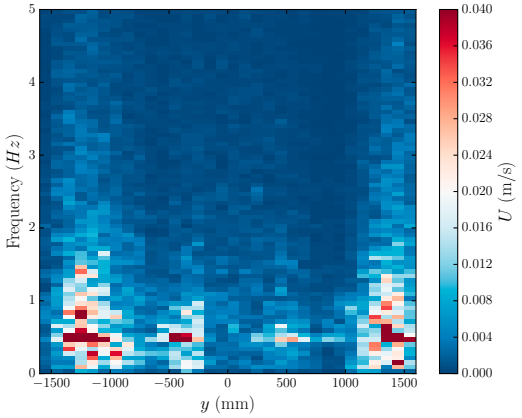

Fig. 13: Spectrogram of the along wind wake velocity U, with imposed surge motion with wake reduced velocity $V_W^* = 1$, at below-rated wind speed

tip distance from the hub; whereas, the lower energy extraction of the rotor from the incoming wind due to lower efficiency at above-rated condition is reflected by the nearly smooth spectral content, Fig.9. Nevertheless, it is worth noticing that at above-rated condition Fig.9, where the wake is less turbulent than at rated Fig.8, it is distinctly visible in the spectrum a line at approximately 4 Hz, which is related at the rotation of the rotor at 240 rpm characteristic of both rated and above rated conditions (Fig.8 and Fig.9). In this regard, the presence of 1P frequency in the spectrum might be linked to the non perfect equality in terms aerodynamic behaviour among the 3 blades (e.g. very small differences in pitch setting moving from below- and rated conditions to the above-rated one).

When it comes to moving the wind turbine model by imposing sinusoidal motion it can be noticed, from Fig.10 and 11, that the mean wind speed in the wake (Fig.7) affects the entity of downwind speed variation U at the frequency of motion. More specifically, Fig.10 and 11 show respectively the velocity U measured downstream at rated and above rated conditions: from each acquisition gathered along the cross-wind direction y only the surge motion frequency was considered from the spectra and re-synchronized in time with respect to the effective wind turbine position by the laser signal, so that to end up with a consistent time-gram as in Fig.10 and 11.

It is visible that the shape of the wake deficit reported in Fig.7 can be seen in Fig.10 and 11 by looking at the amplitude of downwind velocity variation along the cross-wind direction y: the lower the wind velocity in the wake, the lower the velocity variation at the surge motion frequency. Furthermore, it can be noticed that for the above-rated condition, Fig. 11, also the outer positions around the blade tip are characterized by a low in-line wind speed fluctuation at the surge frequency. Therefore two region around the blades tip distance are visible at rated, in Fig.10, whereas one single central region above rated in Fig.11, both consistent with Fig.7. For the specific case of Fig.10 and 11 a surge imposed motion at frequency $f = 0.25$ Hz was imposed at the two wind conditions (see Tab.2).

Fig.12 - Fig.15 report, for below and above rated conditions, a comparison respectively to the high and low "wake reduced frequency" V_W^* dynamic conditions. In Fig.12 - Fig.15 the spectrograms are normalized with respect to the maximum amplitude for a more straightforward comparison. Fig.12 and 13 report the below-rated spectrograms at two different wave reduced velocities V_W^* that, with reference to Tab.2, are related to surge imposed motions respectively at frequencies 0.25 and 1 Hz. Nevertheless, the presence of the motion is visible only for the higher reduced velocity $V_W^* = 4$, linked to the quasi-steady condition, whereas for Fig.12 in the non-linear region of low wake reduced velocity ($V_W^* = 1$) the turbulence due to greater unsteady condition are smeared out more quickly within the wake, not being detected by the downwind anemometers. This confirms the effectiveness of the the parameter V_W^* in the evaluation of the dependency of the unsteady aerodynamics on the dynamics of the floating platform. However, this dependency, as pointed out in [6], is also on the aerodynamic efficiency of the specific operating condition (i.e. C_t, Fig.4): as it can be seen in Fig.14 and 15 the frequencies of motions, respectively 0.25 and 2 Hz are both visible either in the high and the low reduced velocity conditions, differently from what happens for the below rated cases, Fig.12 and 13, suggesting

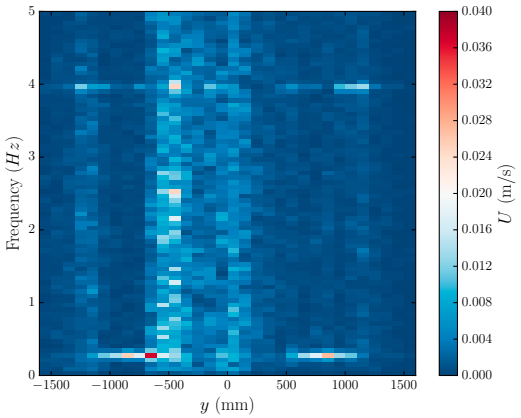

Fig. 14: Spectrogram of the along wind wake velocity U, with imposed surge motion with wake reduced velocity $V_W^* = 9$, at above-rated wind speed

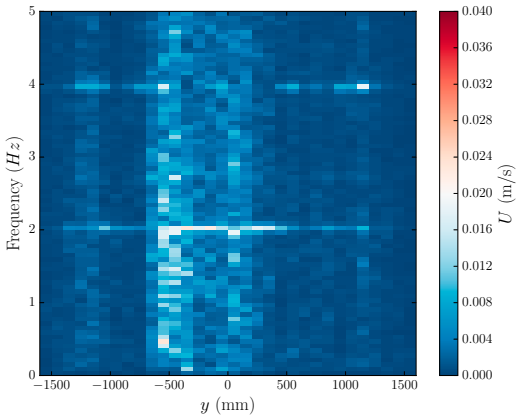

Fig. 15: Spectrogram of the along wind wake velocity U, with imposed surge motion with wake reduced velocity $V_W^* = 1$, at above-rated wind speed

the dual dependency of the wake spectral contents both on the aerodynamic efficiency and the wake reduced velocity.

4. Conclusions and further developments

In this paper a first set of results concerning wake measurements downstream of a floating wind turbine was reported. Measurements of both steady and unsteady conditions were gathered and presented, respectively without and with surge imposed motion of the wind turbine scale model. The former were carried out to check the consistency with literature in this topic and the effectiveness of the measuring approach: more specifically, a 2D map at a distance of 2.3 times the rotor diameter D was obtained at rated wind speed condition. This downwind distance characterized the whole measurement campaign. The wake deficit was computed and compared with the thrust force directly measured by the balance at the nacelle, showing perfect agreement. Furthermore, also the wake velocity at hub height along cross wind direction was measured in steady condition at below- and above-rated wind conditions, showing a very good agreement with the state-of-the art of wind turbine wake knowledge, in terms of the dependency of the wake deficit with the corresponding thrust coefficient Ct at the specific wind turbine operating condition. The same is valid also looking at the corresponding spectra of the cross-wind acquisitions.

Moreover, wake measurements at different operational conditions (e.g. below-, above- and rated wind speed) and different platform surge motion conditions (e.g. amplitude and frequency) were gathered along cross wind direction at hub height. The following main observations can be reported:

- ongoing studies by authors on the unsteady aerodynamics of floating wind turbines led to assume the ”wake reduced velocity” V_W^* as an effective parameter to describe the global aerodynamic unsteady condition of a floating offshore wind turbine: it can be considered as the number of rotor diameters travelled by the single air particle within a complete cycle of (mono-harmonic) platform motion, so that high values of V_W^* means quasi-steady condition, whereas low values are related to greater unsteadiness and non-linearity. This parameter was found to be also representative for this study
- the entity of wind speed fluctuation at the surge motion frequency is dependant on the local wake speed: radial positions with higher wake deficit show lower fluctuation amplitudes
- when the turbine is operating at low Ct (i.e. above rated), the corresponding downwind velocity spectra are quite ”clean” (also the frequencies multiple of the rotational one are clearly visible), and when the surge motion is activated the related frequency is visible either for low and high values of V_W^*

- when the turbine operates at high thrust coefficient Ct values (i.e. below- and rated), the energy extracted from the wind is higher, resulting in a more smeared out spectrum over the frequencies of the downwind speed measurements. When the surge motion is activated, the related frequency is visible in the downwind velocity spectra only for high values of V_W^*

These items can be therefore summarized considering that the wake dynamics of floating wind turbines can be investigated by considering the dual dependency on the aerodynamic efficiency and the "reduced wake velocity" V_W^*, taking into account the machine operational condition as well as the platform frequency motion. These observations need to be consolidated by further tests, possibly carrying out measurements at different downwind distances and also making sure that the dependency on the motion amplitudes can be actually neglected, as assumed in this work.

5. Acknowledgements

This study has partially relied on funds received within LIFES50+ project from European Union's Horizon 2020 research and innovation programme under grant agreement No 640741.

References

[1] Vermeer, L.J., S, J.N., Crespo, A.. Wind turbine wake aerodynamics 2003;39:467–510. doi:10.1016/S0376-0421(03)00078-2.
[2] Sanderse, B.. Aerodynamics of wind turbine wakes: Literature review. Tech. Rep.; Energy Research Center of the Netherlands; 2009.
[3] Bayati, I., Belloli, M., Bernini, L., Fiore, E., Giberti, H., Zasso, A.. On the functional design of the DTU10 MW wind turbine scale model of LIFES50+ project. Journal of Physics: Conference Series 2016;753(5). doi:10.1088/1742-6596/753/5/052018.
[4] Bayati, I., Belloli, M., Bernini, L., Giberti, H., Zasso, A.. On the scale model technology for floating offshore wind turbines. IET Renewable Power Generation 2017;June. doi:10.1049/iet-rpg.2016.0956.
[5] Bayati, I., Belloli, M., Bernini, L., Zasso, A.. Wind tunnel validation of AeroDyn within LIFES50+ project: Imposed Surge and Pitch tests. Journal of Physics: Conference Series 2016;753(9). doi:10.1088/1742-6596/753/9/092001.
[6] Bayati, I., Belloli, M., Bernini, L., Zasso, A.. A Formulation For The Unsteady Aerodynamics Of Floating Wind Turbines, With Focus On The Global Dynamics. In: Proceedings of the International Conference on Offshore Mechanics and Arctic Engineering - OMAE; vol. OMAE2017-61925. 2017,.
[7] Farrugia, R., Sant, T., Micallef, D.. Investigating the aerodynamic performance of a model offshore fl oating wind turbine. Renewable Energy 2014;70(July 2013):24–30. URL: http://dx.doi.org/10.1016/j.renene.2013.12.043. doi:10.1016/j.renene.2013.12.043.
[8] Farrugia, R., Sant, T., Micallef, D.. A study on the aerodynamics of a fl oating wind turbine rotor. Renewable Energy 2016;86:770–784. URL: http://dx.doi.org/10.1016/j.renene.2015.08.063. doi:10.1016/j.renene.2015.08.063.
[9] Micallef, D., Sant, T.. Loading effects on fl oating offshore horizontal axis wind turbines in surge motion. Renewable Energy 2015;83:737–748. URL: http://dx.doi.org/10.1016/j.renene.2015.05.016. doi:10.1016/j.renene.2015.05.016.
[10] Bayo, R., Rockel, S., Peinke, J., Michael, H.. Wake to wake interaction of floating wind turbine models in free pitch motion : An eddy viscosity and mixing length approach 2016;85:666–676. doi:10.1016/j.renene.2015.07.012.
[11] Bak, C.. The dtu 10-mw reference wind turbine. Technical University of Denmark, DTU Wind Energy 2013;.
[12] Bayati, I., Belloli, M., Bernini, L., Mikkelsen, R., Zasso, A.. On the aero-elastic design of the DTU 10MW wind turbine blade for the LIFES50+ wind tunnel scale model. Journal of Physics: Conference Series 2016;753(2). doi:10.1088/1742-6596/753/2/022028.
[13] Bayati, I., Bernini, L., Belloli, M., Zasso, A.. Aerodynamic design methodology for wind tunnel tests of wind turbine rotors. In: Journal of Wind Engineering and Industrial Aerodynamics; vol. June. 2017,doi:10.1016/j.jweia.2017.05.004.
[14] H2020 lifes50+ project. 2016. URL: http://lifes50plus.eu/.
[15] Sauder, T., Chabaud, V., Thys, M., Bachynski, E., Sæther, L.. Real-time hybrid model testing of a braceless semi-submersible wind turbine. Part I: The hybrid approach. In: Proceedings of the International Conference on Offshore Mechanics and Arctic Engineering - OMAE; vol. 6. ISBN 9780791849972; 2016,doi:10.1115/OMAE2016-54435.
[16] Berthelsen, P., Bachynski, E., Karimirad, M., Thys, M.. Real-time hybrid model tests of a braceless semi-submersible wind turbine. Part III: Calibration of a numerical model. In: Proceedings of the International Conference on Offshore Mechanics and Arctic Engineering - OMAE; vol. 6. ISBN 9780791849972; 2016,doi:10.1115/OMAE2016-54640.
[17] Bachynski, E., Thys, M., Sauder, T., Chabaud, V., Sæther, L.. Real-time hybrid model testing of a braceless semi-submersible wind turbine. Part II: Experimental results. In: Proceedings of the International Conference on Offshore Mechanics and Arctic Engineering - OMAE; vol. 6. ISBN 9780791849972; 2016,doi:10.1115/OMAE2016-54437.
[18] Bayati, I., Belloli, M., Ferrari, D., Fossati, F., Giberti, H.. Design of a 6-DoF robotic platform for wind tunnel tests of floating wind turbines. In: Energy Procedia; vol. 53. 2014,doi:10.1016/j.egypro.2014.07.240.
[19] Politecnico di milano. Wind Tunnel. URL: http://www.windtunnel.polimi.it/.
[20] Hansen, M.. Aerodynamics of Wind Turbines: second edition. 2 ed.; Earthscan Publications Ltd; 2008. ISBN 978-1-84407-438-9.